Taylor & Francis
Taylor & Francis Group

Science and Technology for the Built Environment

ISSN: (Print) (Online) Journal homepage: https://www.tandfonline.com/loi/uhvc21

Thermal resistance of ventilated air-spaces behind external claddings; definitions and challenges (ASHRAE 1759-RP)

Mohammad Rahiminejad & Dolaana Khovalyg

To cite this article: Mohammad Rahiminejad & Dolaana Khovalyg (2021): Thermal resistance of ventilated air-spaces behind external claddings; definitions and challenges (ASHRAE 1759-RP), Science and Technology for the Built Environment, DOI: 10.1080/23744731.2021.1898819

To link to this article: https://doi.org/10.1080/23744731.2021.1898819

Published online: 24 Mar 2021.

Science and Technology for the Built Environment, (2021) **0**, 1–18
Published with license by Taylor & Francis
ISSN: 2374-4731 print / 2374-474X online
DOI: 10.1080/23744731.2021.1898819

Thermal resistance of ventilated air-spaces behind external claddings; definitions and challenges (ASHRAE 1759-RP)

MOHAMMAD RAHIMINEJAD* and DOLAANA KHOVALYG

Thermal Engineering for the Built Environment Laboratory (TEBEL), Ecole Polytechnique Fédérale de Lausanne (EPFL), Lausanne, Switzerland

The presence of an air-space within a building envelope is known to have a varying contribution to the overall thermal performance of the wall assembly due to the combined effect of convection and radiation in the air cavity. In particular, the thermal resistance of a ventilated air-space can vary significantly depending on multiple environmental and thermo-physical parameters. Although the thermal resistance of enclosed air-spaces in the building structures has been thoroughly investigated in the literature, it has not been defined for a ventilated cavity. This paper aims to introduce the plausible definitions of the thermal resistance of a vertical ventilated air-space behind external cladding systems. Both theoretical and applied formulations are provided and compared. The energy balance method is used to model the steady-state heat transfer through two types of traditional external wall systems (i.e., brick and vinyl siding) in summer and winter conditions. A range of air exchange rates in the cavity is examined, and the effect of the presence of reflective insulation in the air-space on the thermal resistance of the air gap is analyzed. The results show that the presence of a ventilated cavity in the wall assembly can influence the thermal performance of the building envelope. In particular, the effective thermal resistance of a ventilated air-space behind a brick cladding wall could be between 0.17 and 1.85 times the thermal resistance of the cladding in the range of air change rate in the cavity from 0 to 100 1/h. The effective thermal resistance of the ventilated air gap behind vinyl siding could reach up to 9 times the thermal resistance of the cladding.

Introduction

In recent years, there has been a growing interest in analyzing the thermal characteristics of building envelopes to reduce energy use in buildings since thermal energy losses through the building envelope are responsible for about 50% of all building energy use (Feng, Sha, and Xu 2016). In particular, the properly chosen materials of the external wall can help in saving up to 50–60% energy use of the buildings (Shehadi 2018). Adjacent elements in multi-layered walls can have an impact on the performance of the entire assembly as well. For instance, correctly designed ventilated air cavities behind the exterior cladding systems can contribute toward energy savings in buildings (Aelenei 2006). Reduction in energy use of buildings can be achieved by adopting building envelopes characterized by low thermal transmittance or high thermal resistance value of their elements. The thermal resistance coefficient, known as R-value, is the temperature difference across the element divided by the rate of steady-state or time-averaged heat transfer through one square meter of a building component.

It is becoming more common to construct building walls with a cladding incorporating a ventilated air cavity to control drying due to inward driven vapor from rain wetted absorbent claddings (Straube and Finch 2009). Figure 1 shows illustrations for the two common ventilated wall assemblies (i.e., brick and vinyl siding). The use of large ventilated cavities has already been required by some building codes (NBCC 2005). Several research projects have analyzed different hygrothermal aspects of the ventilated cavity incorporated in the exterior surface of the wall assemblies (Finch and Straube 2007; Balocco 2009; Manuel et al. 2013; Langmans and Roels 2015; Van Belleghem et al. 2015; Gagliano, Nocera, and Aneli 2016; Buratti et al. 2018, Meyer et al. 2019; Tariku and Iffa 2019). A very comprehensive literature review on the factors affecting the airflow rate in the ventilated cavity behind different types of traditional external cladding systems is recently performed by Rahiminejad and Khovalyg (2021). The expected ventilation rates in the air-spaces behind several exterior façades are

Received September 06, 2020; Accepted March 01, 2021
Mohammad Rahiminejad is a Doctoral Assistant. **Dolaana Khovalyg**, Associate Member ASHRAE, is an Assistant Professor.
Corresponding author e-mail: mohammad.rahiminejad@epfl.ch

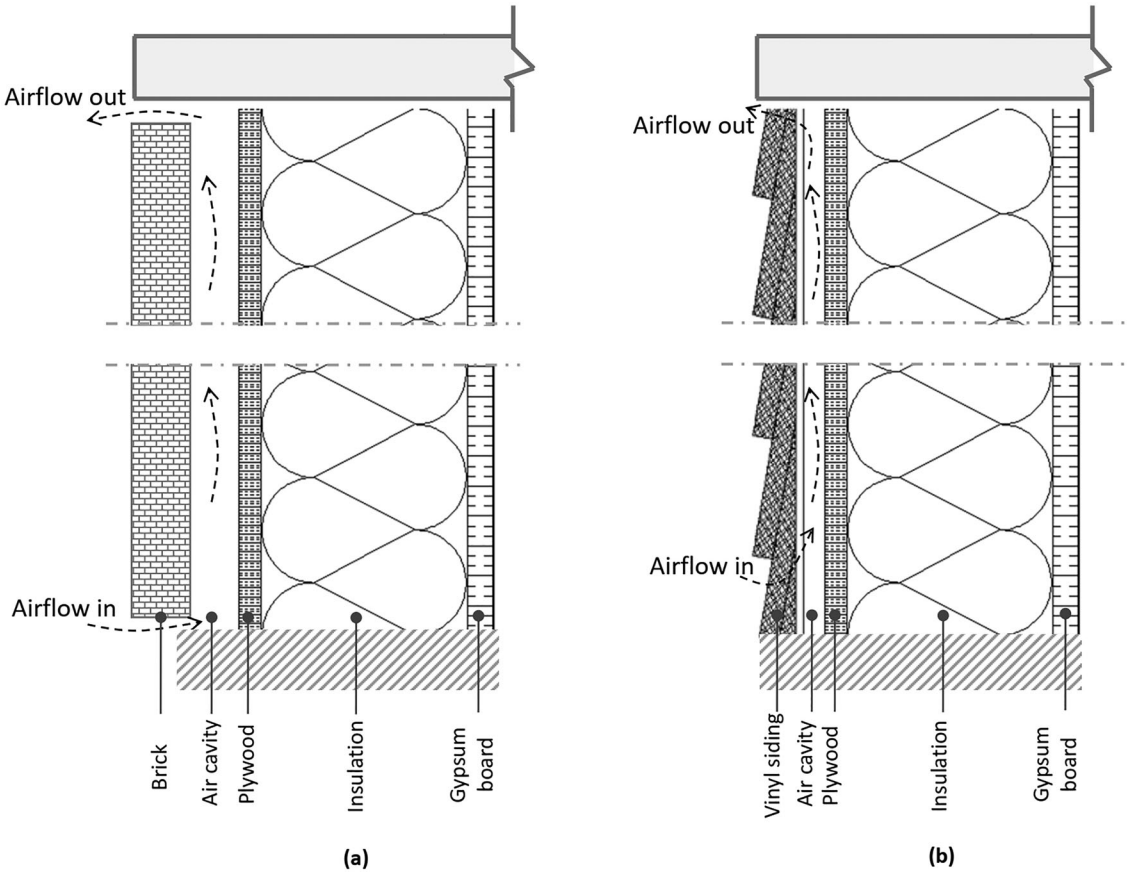

Fig. 1. Cross-sections of typical ventilated wall assemblies: (a) brick veneer, (b) vinyl siding.

collected through the literature. The complexity of the airflow in ventilated air cavities is shown to be a result of the balance between driving forces (wind effect and stack effect) and the pressure resistance along the air passage. According to this review paper that considered different cladding systems, the average value for air change rate per hour behind various types of external facades stays lower than 1000 1/h (Rahiminejad and Khovalyg 2021).

The definition of the thermal resistance of enclosed air-spaces is not a new concept, and the ASHRAE Handbook of Fundamentals (HOF) (2009) provisions are based on testing and research data presented by Robinson, Powlitch and Dill (1954). Despite the prevalence of several studies on the airflow behavior in an enclosed air-space (Desjarlais and Yarbrough 1991; Saber 2012; Bekkouche et al. 2013; Saber 2013a, 2013b), research to quantify the thermal performance of ventilated air-cavities behind external cladding systems is still lacking. In particular, the thermal resistance of a ventilated cavity incorporated in a wall assembly has not been identified in the previous publications. The scarcity of thermal performance data and test methods acts as a barrier to reliable guidance and wide adoption of wall assemblies that include air-cavities behind the cladding. As stated in the ASHRAE HOF (2009), all the available information we have on thermal resistances applies for ideal conditions, i.e., air-spaces of uniform thickness bounded by plane, smooth, parallel surfaces with no air-leakage to or from the space. While it is accepted that all insulation materials are affected to some extent by air-leakage (Schumacher et al. 2013), there is little information available to quantify the air-leakage impact in applications where airflow is expected to occur, such as air-spaces behind air-permeable and vented/ventilated cladding systems. Considering another international standard, EN ISO 6946 (2007) provides a steady-state calculation method for the total thermal resistance of a building component containing a well-ventilated air layer that is based on disregarding the thermal resistance of the air layer and all other layers between the air layer and external environment, and including an external surface resistance corresponding to still air. The method excludes doors, windows, and other glazed units, curtain walling, components that involve heat transfer to the ground, and air-permeable components. However, the research basis is not reported, and guidance is vague and cannot be incorporated into practical building design and code applications. Therefore, descriptions of the thermal resistance of a ventilated cavity in the current standards are inadequate. Even if this concept has been considered in a standard such as EN ISO 6946 (2007), the explanation is based on static consideration, and the dynamic variation of the thermal resistance is not acknowledged.

In the present study, three plausible definitions of the thermal resistance of the ventilated air gap are described and compared. Firstly, a theoretical definition is introduced based on the non-linear network of thermal resistances within the wall assembly. Due to the complexity of the airflow behavior in the air gap and its dependence on multiple parameters, the theoretical expression of the thermal resistance of the

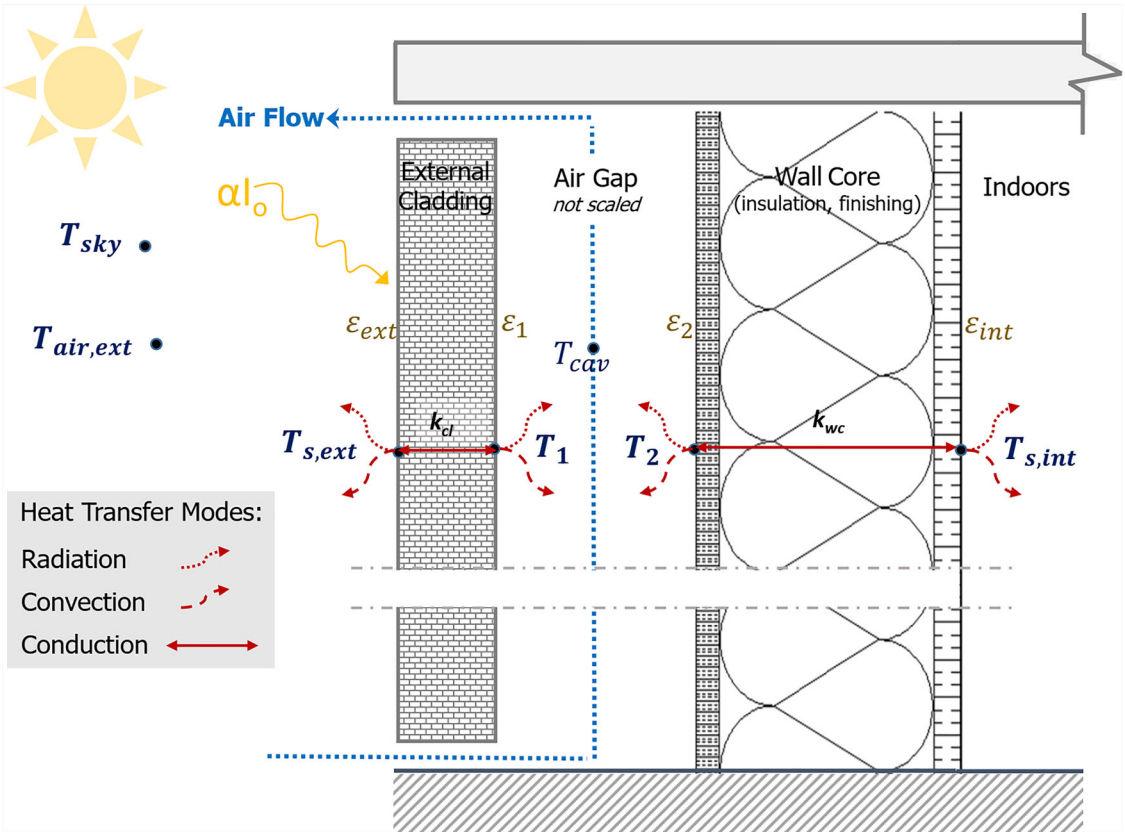

Fig. 2. Heat transfer mechanisms in a ventilated wall cavity (source: Authors).

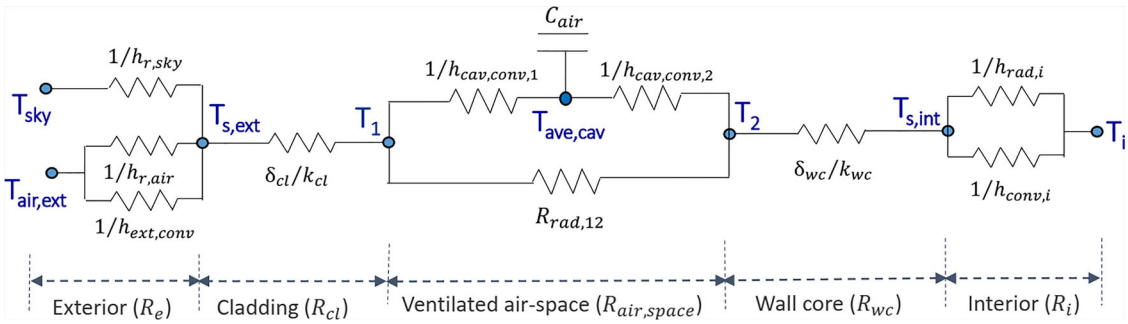

Fig. 3. The overall network of thermal resistances for heat transfer across the vertical ventilated wall.

ventilated air gap is not straightforward to use in practice. Therefore, two practical definitions of the ventilated air gap thermal resistance, *apparent* and *effective*, for conditions with no solar flux are introduced. To simulate a ventilated wall structure, a numerical code is developed for steady-state heat flow in the wall assembly based on the energy balance method through the entire geometry. The model is validated against the actual hot box test results available in the literature. Thereafter, two external cladding types (i.e., brick and vinyl siding) are considered, and the impact of the air exchange rate, outdoor temperature, and presence of reflective insulation on the variation of the thermal resistance of the ventilated air-space per each definition is investigated. Finally, more analysis is performed for the definition of the thermal resistance of a ventilated air-space that is more convenient for conventional engineering practices.

Theoretical background

To advance understanding of the effect of a ventilated air gap on the thermal performance of the wall assembly, first of all, it is necessary to evaluate temperatures and heat fluxes in and out of the air gap. Therefore, an analytical workflow in the steady-state condition was developed by considering the energy balance equations in the ventilated wall assembly.

Energy balance

An illustration of the heat transfer mechanisms across a ventilated wall assembly is shown in Figure 2. The overall network of thermal resistances across the wall assembly is illustrated in Figure 3. Radiation and convection act on each surface, while conduction takes place in solid materials such as cladding and wall core. It should be noted that there are radiation and conduction through the insulation, usually modeled as apparent diffusion (Mathes, Blumenberg, and Keller 1990). However, only the effective conduction part is considered in this study for simplicity. Combined heat transfer on the external side of the cladding can be expressed by the thermal resistance R_{ext}, while the heat transfer on the internal side of the wall core can be expressed as R_{int}. Conduction through the cladding is indicated using R_{cl}, while conduction through the wall core is indicated using R_{wc}. The temperature in the centerline of the air gap is indicated as T_{cav}. Temperatures and heat fluxes at each surface and temperature of the airflow and its enthalpy can be determined by considering an energy balance at each surface.

Further details of defining energy balance on each surface are provided per unit of width of the façade considering the following assumptions:

- All surface temperatures (i.e., the exterior surface of the cladding, the interior surface of the wall core, and cavity walls) have no significant variations along with the height of the wall—the temperature of each surface is assumed to be uniform along with the height.
- Although the air temperature changes along with the height of the channel, the heat exchange is modeled by averaging the temperature along the channel.
- The effect of the thermal mass of the solid materials is not considered.
- Airflow inside the air gap is hydro-dynamically and thermally fully developed.
- Slot openings with uniform inlet and outlet geometries are considered.
- External cladding and the wall core are impermeable (i.e., the effect of the airflow through permeable walls of the ventilated cavity is not considered in the analysis of the thermal resistance of the ventilated cavity).
- The effect of thermal bridges across a ventilated air cavity is not considered.

Energy balance of the air cavity

Assuming a differential control volume in the air cavity (Figure 4), the energy balance includes the following terms:

- Change in the internal energy of the air content of the differential volume:

$$dq_{cav} = \rho_{cav} \cdot C_{p_{cav}} \cdot d_{cav} \cdot u_m \cdot dT_{cav} \tag{1}$$

- Convective heat exchange with external cladding (left cavity wall):

$$dq_{cav,conv,1} = h_{cav,conv,1} \cdot (T_1 - T_{cav}) \cdot dy \tag{2}$$

- Convective heat exchange with the wall core (right cavity wall):

$$dq_{cav,conv,2} = h_{cav,conv,2} \cdot (T_2 - T_{cav}) \cdot dy \tag{3}$$

- Radiative heat exchange between left and right cavity walls:

$$dq_{rad,12} = h_{rad,12} \cdot (T_1 - T_2) \cdot dy \tag{4}$$

- Radiative heat exchange between right and left cavity walls:

$$dq_{rad,21} = h_{rad,12} \cdot (T_2 - T_1) \cdot dy \tag{5}$$

The balance of each contribution is the following:

$$\rho_{cav} \cdot C_{p_{cav}} \cdot d_{cav} \cdot u_m \cdot dT_{cav} + h_{cav,conv,1} \cdot (T_1 - T_{cav}) \cdot dy + h_{cav,conv,2} \cdot (T_2 - T_{cav}) \cdot dy = 0 \tag{6}$$

Thus:

$$\frac{dT_{cav}}{dy} - \left(\frac{h_{cav,conv,1} + h_{cav,conv,2}}{\rho_{cav} \cdot C_{p_{cav}} \cdot d_{cav} \cdot u_m}\right)\left[T_{cav} - \frac{h_{cav,conv,1} \cdot T_1 + h_{cav,conv,2} \cdot T_2}{h_{cav,conv,1} + h_{cav,conv,2}}\right] = 0 \tag{7}$$

We can define two variables L_o and T_{eq} as:

$$\frac{h_{cav,conv,1} + h_{cav,conv,2}}{\rho_{cav} \cdot C_{p_{cav}} \cdot d_{cav} \cdot u_m} = \frac{1}{L_0} \tag{8}$$

$$\frac{h_{cav,conv,1} \cdot T_1 + h_{cav,conv,2} \cdot T_2}{h_{cav,conv,1} + h_{cav,conv,2}} = T_{eq} \tag{9}$$

Variation of the air temperature along the *y-axis* can be defined by the integration of Equation (7) over the height of the cavity:

$$\boldsymbol{T_{cav}(y) = T_{eq} - (T_{eq} - T_{en}).e^{-\frac{y}{L_0}}} \tag{10}$$

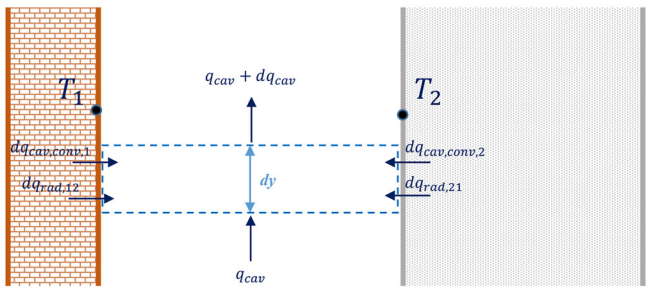

Fig. 4. Differential control volume in the cavity.

where T_{en} is the air temperature at the entrance of the cavity, that is assumed to be equal to the outdoor temperature ($T_{en} \cong T_{air,ext}$). Since it is necessary to know the temperature of the walls T_1 and T_2 to calculate T_{eq}, it is required to consider the energy balance at each wall surface to determine the expression for T_1 & T_2.

Energy balance on the left-side cavity wall (external cladding)

Assuming a differential control volume for the left surface of the cavity, three terms for the energy balance are the following:

- Convective heat exchange between the airflow and the left wall:

$$dq_{cav,conv,1} = h_{cav,conv,1} \cdot (T_1 - T_{cav}) \cdot dy \tag{11}$$

- Radiative heat exchange between two walls bounding the air gap:

$$dq_{rad,12} = h_{rad,12} \cdot (T_1 - T_2) \cdot dy \tag{12}$$

- Heat transfer due to conduction through the external cladding:

$$dq_{cond,cl} = \frac{T_1 - T_{s,ext}}{R_{cl}} \cdot dy \tag{13}$$

The energy balance on the left wall of the air gap is the following:

$$h_{cav,conv} \cdot (T_1 - T_{cav}) \cdot dy + h_{rad,12} \cdot (T_1 - T_2) \cdot dy + \frac{T_1 - T_{s,ext}}{R_{cl}} \cdot dy = 0 \tag{14}$$

By rearranging Equation (14), the temperature of the wall T_1 can be expressed as:

$$\boldsymbol{T_1 = \frac{h_{cav,conv} \cdot T_{cav} + h_{rad,12} \cdot T_2 + \frac{T_{s,ext}}{R_{cl}}}{h_{cav,conv} + h_{rad,12} + \frac{1}{R_{cl}}}} \tag{15}$$

To define the outdoor surface temperature $T_{s,ext}$ (highlighted in red), the energy balance at the exterior surfaces needs to be analyzed.

Energy balance at the exterior surface of cladding (outdoors)

The exterior surface of the cladding is exposed to solar radiation, radiation with the sky, and with the ambient air. The convection heat transfer occurs with the outdoor, while conduction also causes heat transfer in the cladding. The heat transfer components are as follow:

- Radiation heat exchange has two main parts in the long-wavelength region:
  - Exchange with the sky:

$$dq_{r,sk} = h_{r,sk}(T_{sk} - T_{s,ext}) \cdot dy \tag{16}$$

  - Exchange with the surroundings (ground and other buildings; the outside dry air temperature is assumed for this mass):

$$dq_{r,air} = h_{r,air}(T_{air,ext} - T_{s,ext}) \cdot dy \tag{17}$$

  - Heat flow received by the external surface depends on the incident radiation and the absorption coefficient in the short wavelength region due to the incident solar heat flux:

$$dq_{solar} = I\alpha \cdot dy \tag{18}$$

- Convective heat exchange of the surface with the outside air:

$$dq_{ext,conv} = h_{ext,conv}(T_{air,ext} - T_{s,ext}) \cdot dy \tag{19}$$

- Conduction heat exchange through the cladding material:

$$dq_{cond,cl} = \frac{(T_1 - T_{s,ext})}{R_{cl}} \cdot dy \tag{20}$$

The external surface temperature of the cladding can be found by solving the energy balance:

$$h_{r,sk}(T_{sk} - T_{s,ext}) + h_{r,air}(T_{air,ext} - T_{s,ext}) + I\alpha + h_{ext,conv}(T_{air,ext} - T_{s,ext}) + \frac{(T_1 - T_{s,ext})}{R_{cl}} = 0 \tag{21}$$

$$\boldsymbol{T_{s,ext} = \frac{I\alpha + h_{r,sk}T_{sk} + h_{r,air}T_{air,ext} + h_{ext,conv}T_{air,ext} + \frac{T_1}{R_{cl}}}{h_{r,sk} + h_{r,air} + h_{ext,conv} + \frac{1}{R_{cl}}}} \tag{22}$$

Energy balance on the right-side cavity wall (wall core)

Assuming a control volume for the right surface of the cavity, the terms for the energy balance are:

- Convective heat exchange between the airflow and the right wall:

$$dq_{cav,conv,2} = h_{cav,conv,2} \cdot (T_2 - T_{cav}) \cdot dy \tag{23}$$

- Radiative heat exchange between two walls bounding the air gap:

$$dq_{rad,21} = h_{rad,12} \cdot (T_2 - T_1) \cdot dy \tag{24}$$

- Heat transfer due to conduction through the wall core:

$$dq_{cond,wc} = \frac{T_2 - T_{s,int}}{R_{wc}} \cdot dy \tag{25}$$

The energy balance on the right wall:

$$h_{cav,conv} \cdot (T_2 - T_{cav}) \cdot dy + h_{rad,12} \cdot (T_2 - T_1) \cdot dy + \frac{T_2 - T_{s,int}}{R_{wc}} \cdot dy = 0 \tag{26}$$

By rearranging Equation (26), the temperature of the wall T_2 can be determined as:

$$\boldsymbol{T_2 = \frac{h_{cav,conv} \cdot T_{cav} + h_{rad,12} \cdot T_1 + \frac{T_{s,int}}{R_{wc}}}{h_{cav,conv} + h_{rad,12} + \frac{1}{R_{wc}}}} \tag{27}$$

To define the indoor surface temperature $T_{s,int}$ (highlighted in red), energy balance at the interior surfaces needs to be considered.

Energy balance at the interior surface of the wall core (indoors)

By assuming a control volume for the interior surface, we will have only convective and conductive heat transfer terms:

- Convective heat exchange with the interior area:

$$dq_{int,conv} = h_{int,conv} \cdot (T_{s,int} - T_i) \cdot dy \quad (28)$$

- Radiative heat exchange with the interior area (the interior dry air temperature is assumed for the surrounding):

$$dq_{int,rad} = h_{int,rad} \cdot (T_{s,int} - T_i) \cdot dy \quad (29)$$

- Conductive heat exchange in the wall core:

$$dq_{cond,wc} = \frac{T_{s,int} - T_2}{R_{wc}} \cdot dy \quad (30)$$

Therefore:

$$\boldsymbol{T_{s,int}} = \frac{(\boldsymbol{h_{int,conv}} + \boldsymbol{h_{int,rad}}) \cdot \boldsymbol{T_i} + \frac{\boldsymbol{T_2}}{\boldsymbol{R_{wc}}}}{(\boldsymbol{h_{int,conv}} + \boldsymbol{h_{int,rad}}) + \frac{1}{\boldsymbol{R_{wc}}}} \quad (31)$$

Heat transfer correlations

Before introducing heat transfer correlations used in the analytical solution for the ventilated wall assembly, it is necessary to define key parameters used to characterize the phenomena.

- The hydraulic diameter of the cavity is calculated based on the rectangular duct flow (Falk and Sandin 2013) which could be considered as a parallel flow at a high aspect ratio (Straube 1998):

$$d_H = \begin{cases} \frac{2 \cdot d_{cav} \cdot w}{d_{cav} + w} & for\ rectangular\ duct\ flow \\ 2 \cdot d_{cav} & for\ parallel\ plate\ flow \end{cases} \quad (32)$$

- Reynolds number based on the width of the air gap d_{cav} :

$$Re_H = \frac{\rho_{cav} \cdot u_m \cdot d_{cav}}{\mu} \quad (33)$$

- Mean air velocity in the cavity calculated from the given ACH and the height of the air-space:

$$u_m = \frac{ACH \cdot H}{3600} \quad (34)$$

- Convective heat transfer coefficients

At the outdoor surface: Convection at the exterior surface always combines free and forced convection, and the latter is a function of the wind speed. To determine the exterior convective heat transfer coefficient, a well-known equation by Nusselt and Jurges (1922) used in studies of building envelope energy systems' modeling by Manuel et al. (2013), Skoplaki and Palyvos (2009), Balocco (2002), and Holman (1991) was applied:

$$h_{ext,conv} = 5.7 + 3.8 \cdot V_{wind}, where [V] = m/s \quad (35)$$

At the indoor surface: The overall thermal resistance for the interior vertical surface is considered as 0.68 hr· ft^2· F/BTU (0.12 m^2· K/W) based on the standard ASHRAE 90.1-2016 (ASHRAE Standard 2016).

Inside the air gap: Convective heat transfer inside the ventilated air gap plays a predominant role in defining the heat flow across the air gap. Thus, the use of the appropriate correlation is important to estimate correctly the heat transfer due to the airflow. Manuel et al. (2013) proposed a correlation for a ventilated cavity and validated the formula with experimental measurements. The formulas below correspond to each surface of the air gap (the left surface has a subscript of "1" and the right surface is "2").

$$h_{cav,conv,1} = 0.85\left[1.959 + 1.517\left(|T_1 - T_{ave,cav}|\right)^{\frac{1}{3}} + 1.33u_m\right], \quad where\ [T]\ in\ K \quad (36)$$

$$h_{cav,conv,2} = 0.85\left[1.959 + 1.517\left(|T_2 - T_{ave,cav}|\right)^{\frac{1}{3}} + 1.33u_m\right], \quad where\ [T]\ in\ K \quad (37)$$

- Radiative heat transfer coefficients

Between outdoor environment and the external surface of the cladding: The radiation from the sky and surrounding surfaces can be calculated using the equations provided below from Manuel et al. (2013) where temperatures should be in units of Kelvin:

$$h_{rad,air} = F_{s,ext-air} . \varepsilon_{s,ext} . \sigma (T_{air,ext} + T_{s,ext}) . \left(T_{air,ext}^2 + T_{s,ext}^2\right) \quad (38)$$

$$h_{rad,sky} = F_{s,ext-sky} . \varepsilon_{s,ext} . \sigma (T_{sk} + T_{s,ext}) . (T_{sk}^2 + T_{s,ext}^2) \quad (39)$$

The outdoor radiative coefficients depend on temperatures T_{sky}, $T_{s,ext}$, Boltzmann constant σ, emissivity at long wavelengths of the external surface of the cladding $\varepsilon_{s,ext}$, and a view factor $F_{s,ext\text{-}sky}$ usually took as 0.5 in open spaces and urban boundaries as 0.3535 according to Richman and Pressnail (2009). The sky temperature is defined by Duffie and Beckman (2013) with a simple expression:

$$T_{sk} = T_{air,ext} - 6 \quad (40)$$

Between the walls of the ventilated air gap: As for the radiation coefficient, since in building applications the horizontal dimension of the air volume is limited (a few centimeters) compared to the width and the length of the wall (meters), the view factor between the vertical faces could be considered equal to 1 (Baldinelli 2010), therefore the radiation heat transfer coefficient between two walls of the cavity is defined as (Falk and Sandin 2013):

$$h_{rad,12} = 4.\varepsilon_{12}.\sigma.\left(\frac{T_1 + T_2}{2}\right)^3, where\ [T]\ in\ K \quad (41)$$

where T_1andT_2 are cavity walls temperatures which can be defined from Equations (15) and (27).

Validation

Computational method

Based on the analytical solution using the description presented above, a MATLAB® code was developed to calculate temperatures and heat flow according to the flow chart shown in Figure 5. The major part of the code is the procedure of defining the air temperature profile along with the height of the cavity. Since this profile depends on the initially unknown wall temperatures of the wall, one must follow an iterative computational procedure. These two

unknown temperatures are also a function of the air cavity temperature. Therefore, by assuming initial constant temperature along with the height of the cavity walls and by guessing average air temperature in the cavity, the temperature profile in the cavity can be iteratively computed. This iteration process continues until the integrated temperature of the air cavity does not change compared to the value in the previous iteration (the criteria for the difference is < 0.0001).

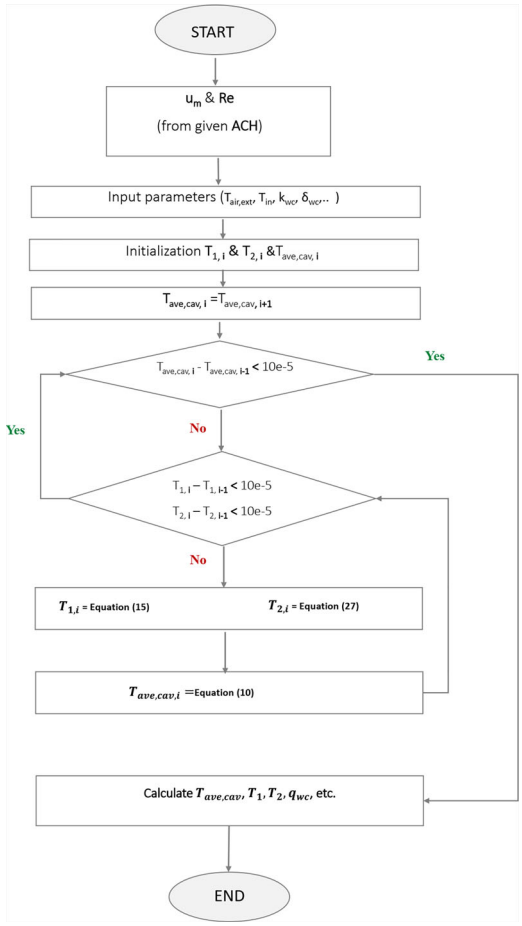

Fig. 5. Flow chart for the analytical solution.

Validation using hot box test results

Verification and validation are important components of any model development. To validate the analytical solution, computed temperatures of surfaces were compared with the results of two hot-box tests referenced in the work statement of 1759-RP (Meyer et al. 2019; EXOVA Test Report 2011). The testing by Meyer et al. (2019) considered brick cladding with a 0.07 m/s forced ventilation airflow behind the brick veneer. EXOVA tested vinyl siding with a conventional hot-box test using a mixing fan airflow applied to an exterior side of the assembly. In contrast to the test performed by Meyer et al. (2019), no forced ventilation air-flow behind the siding was applied. Thus, the airflow behind the vinyl siding only occurs as a result of mixing fan-induced airflow over the surface of the vinyl siding.

Test for the brick veneer external cladding

The thermal performance of various wall constructions was studied and reported by Meyer et al. (2019). The influence of the effective emissivity of weather resistance barriers in wall cavities on the thermal performance of the wall assemblies was tested. The procedure of testing is elaborated in ASTM 1363-05 test report (2009). Input data from the test report are listed in Table 1 and the results of the analytical solution are in Table 2. After evaluating the data available in the report, the following assumptions were used as input data for the computational code:

- The mean air velocity in the cavity is assumed to be equal to the reported airflow
- Values for the cavity geometry (i.e., thickness, height, width) and walls configuration (i.e., external cladding thickness, internal layers (wall core) thickness) are extracted from the illustration in the report

Table 1. Parameters of the hot box in ASTM 1363-05 test report (2009).

Parameter	Units (IP; SI)	Value
u_m	ft/s (m/s)	0.23 (0.07)
d_{cav}	ft (m)	0.06 (0.019)
H	ft (m)	8 (2.44)
w	ft (m)	8 (2.44)
V_{wind}	ft/s (m/s)	17.6 to 21.9 (5.36 to 6.7)
$T_{air,ext}$	°F (°C)	25 (−3.9)
T_i	°F (°C)	100 (+37.8)
ε_1	–	0.9
ε_2	–	0.2
δ_{cl}	ft (m)	0.3 (0.09)
δ_{wc}	ft (m)	0.04 (0.0127) OSB + 0.3 (0.09) Fiberglass + 0.04 (0.0127) Gypsum
k	BTU/(hr · ft · F) [W/(m · K)]	0.56 (0.97) Red brick, 0.08 (0.13) OSB, 0.02 (0.04) Fiberglass, 0.10 (0.17) Gypsum
$T_{s,ext}$	°F (°C)	25.45 (−3.64)
T_1	°F (°C)	27.22 (−2.66)
T_2	°F (°C)	37.64 (+3.13)
$T_{s,int}$	°F (°C)	97.42 (+36.34)

Table 2. Comparison of the computed and measured surface temperatures.

	Test report		Computed results		
Parameter	°F	K	°F	K	Deviation* (%)
$T_{s,ext}$	25.45	269.51	25.77	269.69	0.067
T_1	27.21	270.49	27.64	270.73	0.089
T_2**	37.63	276.28	36.16	275.46	0.297
$T_{s,int}$	97.41	309.49	97.14	309.34	0.048

*The deviation is calculated for absolute temperature scales (in Kelvin).
**Assumed to be equal to the measured temperature behind the building wrap (e = 0.2).

- Thermal conductivities of the materials considered are following: brick 0.56 BTU/hr· ft· F (0.97 W/m· K), OSB 0.08 BTU/hr· ft· F (0.13 W/m· K), fiberglass: 0.02 BTU/hr· ft· F (0.04 W/m· K), gypsum board 0.10 BTU/hr· ft· F (0.17 W/m· K)
- The mean exterior air velocity is considered as the local wind speed [19.7 ft/s (6 m/s)]
- There is no incident solar radiation on the external surface of the cladding
- The emissivity of cavity surfaces is equal to 0.9 and 0.2 (right cavity wall covered by a building wrap).
- Temperatures ($T_{s,ext}$, $T_1, T_2, T_{s,int}$) are averaged from the measured values of middle thermocouples (locations 8, 10, 12, 14 provided in the ASTM 1363-05 test report (2009)).
- Airflow velocity for test #10 was not available, therefore, data from test #9 was used.

According to the results presented, temperatures are very well estimated by the computational workflow developed. The model agrees with the experimental data with an average deviation of ±0.12% in K, showing that it can predict the results in an acceptable range. Although the presence of the brick ties and studs might affect the airflow pattern and also create thermal bridges in the air cavity, the numerical code simply represents temperatures of surfaces between the studs.

Test for the vinyl siding cladding (EXOVA report)

The EXOVA report (EXOVA Test Report 2011) presents the testing of the vinyl siding wall assembly in the hot box apparatus and estimation of the thermal resistance of the air gap using a sequential approach with four wall configurations. The summary of the tests is the following:

- The first (#1) and second (#2) configurations did not include any external cladding and no air gap; the outer surface started from OSB sheathing. The only difference between these assemblies is that a house wrap is added to the second configuration.
- The following two configurations (#3 and #4) used vinyl siding as an external cladding. Configuration #3 had reflective insulation, and it was tested at three different exterior side perpendicular air velocity. The reflective insulation was not used in configuration #4. By examining the cross-sections of the wall assembly presented in the EXOVA report, geometrical data for the wall assembly was retrieved
- Since air gap thickness was not visible in the illustrations of the wall assembly, it was assumed as 0.03 ft (0.009 m), which is a value typical for vinyl sidings
- The profile depth of the vinyl siding was taken as 0.04 ft (0.012 m)
- The mean air velocity inside the cavity was not provided in the report; therefore, it was assumed to be equal to the air velocity on the exterior side
- Thermal conductivities of the materials were considered as follow: Vinyl Siding: 0.06 BTU/hr· ft· F (0.19 W/m· K), Fiberglass: 0.01 BTU/hr· ft· F (0.04 W/m· K), Gypsum Board: 0.05 BTU/hr· ft· F (0.17 W/m· K)
- There was no solar radiation acting on the external surface of the external cladding (I = 0)
- The emissivity of cavity surfaces was 0.9 for the left cavity wall (the inner side of the cladding), and 0.05 for the right cavity wall (the outer side of the wall core) in the presence of the reflective insulation (configuration #3).

A summary of the input parameters is provided in Table 3. Only external $T_{s,ext}$ and internal surface $T_{s,int}$ temperatures were provided in the report. Thus, the results of the analytical solution were compared with these temperatures. Since the effect of solar radiation cannot be tested in the hot box method, there should not be a significant effect of the buoyancy force. Thus, the forced convection correlation presented in section 0 could be applied to evaluate the heat transfer in the wall assembly. However, to compare the magnitude of the difference in the results using forced convection and mixed convection correlation that accounts for the buoyancy force, analytical results were computed considering both correlations. The comparison of the results with the test results is provided in Table 4. According to the comparison, surface temperatures are very well estimated by the analytical solution developed. Although the presence of the anchors and junctions in practice might result in thermal bridges and non-uniform temperature distribution in the wall assembly, the results of the simplified analytical solution have a good agreement with the test results. The maximum deviation between the calculated and measured values reaches 5.55% (in °F; or 3.81% in °C) which occurs in test #5 within configuration #3. This is mainly due to the high airspeed considered in the exterior side of the cavity which is assumed to be the same in the cavity.

The uncertainty of the measurements is not reported, however, the model agrees with the experimental data ±0.32% on average, showing that it can predict the surface temperatures in an acceptable range.

Definitions of the thermal resistance of the ventilated cavity

To properly evaluate the thermal resistance of ventilated airspace for energy code compliance purposes required by

Table 3. Data available from the EXOVA Test Report (2011).

Parameter [units]	Configuration #3			Configuration #4
	Test #3	Test #4	Test #5	Test #6
u_m [ft/s (m/s)]	9.02 (2.75)	1.64 (0.5)	18.04 (5.5)	9.02 (2.75)
d_{cav} [ft (m)]	0.03 (0.009)	0.03 (0.009)	0.03 (0.009)	0.03 (0.009)
H [ft (m)]	8.01 (2.44)	8.01 (2.44)	8.01 (2.44)	8.01 (2.44)
w [ft (m)]	8.01 (2.44)	8.01 (2.44)	8.01 (2.44)	8.01 (2.44)
V_{wind} [ft/s (m/s)]	9.02 (2.75)	1.64 (0.5)	18.04 (5.5)	9.02 (2.75)
$T_{air,ext}$ [°F (**°C**)]	50 (10)	50 (10)	50 (10)	50 (10)
T_i [°F (**°C**)]	100.40 (38)	100.40 (38)	100.40 (38)	100.40 (38)
ε_1	0.9	0.9	0.9	0.9
ε_2	0.05	0.05	0.05	0.9
δ_{cl} [ft (m)]	0.04 (0.012)	0.04 (0.012)	0.04 (0.012)	0.04 (0.012)
δ_{wc} [ft (m)]	0.04 (0.012) OSB + 0.33 (0.101) Fiberglass + 0.04 (0.012) Gypsum			
$T_{s,\ ext}$ [°F (**°C**)]	50.18 (10.10)	50.65 (10.36)	50.22 (10.12)	50.99 (10.55)
T_1 [°F (**°C**)]	–	–	–	–
T_2 [°F (**°C**)]	–	–	–	–
$T_{s,\ int}$ [°F (**°C**)]	96.28 (35.71)	96.31 (35.73)	96.24 (35.69)	96.13 (35.63)

Table 4. Comparison of surface temperatures with the EXOVA test (2011) results.

Parameter	Test results		Computed results		Deviation* (%)
	°F	K	°F	K	
Configuration #3, Test #3					
$T_{s,\ ext}$	50.18	283.25	49.91	283.10	0.05
$T_{s,\ int}$	96.28	308.86	97.72	309.76	0.29
Configuration #3, Test #4					
$T_{s,\ ext}$	50.65	283.51	50.70	283.54	0.01
$T_{s,\ int}$	101.71	311.88	98.06	309.85	0.65
Configuration #3, Test #5					
$T_{s,\ ext}$	50.22	283.27	49.93	283.11	0.06
$T_{s,\ int}$	101.64	311.84	97.84	309.73	0.68
Configuration #4, Test #6					
$T_{s,\ ext}$	50.99	283.70	50.13	283.22	0.17
$T_{s,\ int}$	101.53	311.78	97.84	309.73	0.66

*The deviation is calculated for absolute temperature scales (in Kelvin).

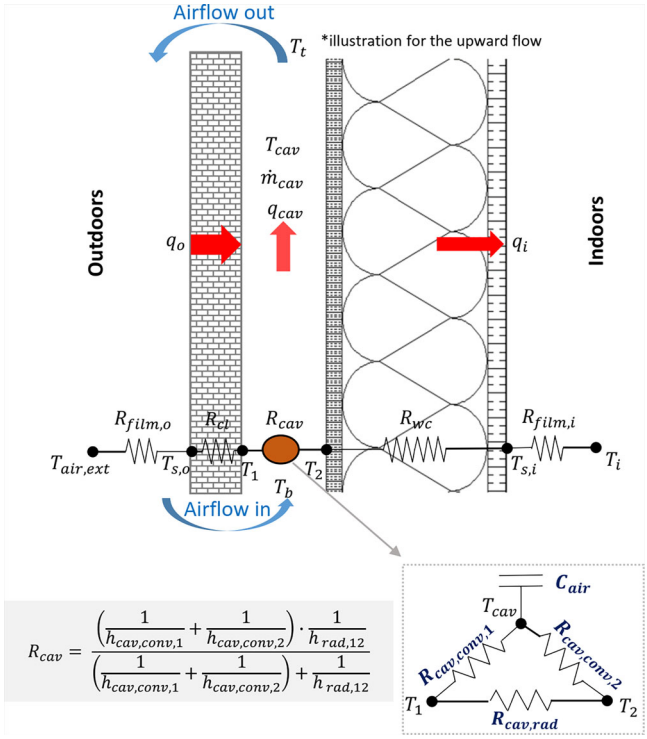

Fig. 6. *Thermal resistance* (R_{cav}) based on the non-linear network of thermal resistances (Method 1) with q_i determined based on the energy balance to account for ventilated airflow heat transfer (summer condition is shown) (source: Authors).

ASHRAE 90.1, this section presents and compares three definitions of thermal resistance of the ventilated air gap and their comparison:

- "***Thermal resistance***" (**R_{cav}**) is defined based on a *non-linear* network of thermal resistances. The illustration is provided in Figure 6, and the method of defining R_{cav} is referred to hereafter as Method 1.
- "***Apparent thermal resistance***" (**$R_{cav,app}$**) is defined based on the *energy balance*. The illustration is provided in Figure 7, and the method of defining $R_{cav,app}$ is referred hereafter as Method 2.
- "***Effective thermal resistance***" (**$R_{cav,eff}$**) is defined based on a *linear network* thermal resistances in an analogy with a closed cavity thermal resistance. The illustration is provided in Figure 8, and the method of defining $R_{cav,eff}$ is referred to hereafter as Method 3. In a simplified analysis of thermal resistances summation, $R_{cav,eff}$ cannot be separately analyzed due to ventilation air flows occurring within an assembly. Thus, $R_{cav,eff}$ is calibrated to produce the same q_i through the wall core assembly as determined with ventilation airflow in the cavity. Consequently, the heat transfer effect of

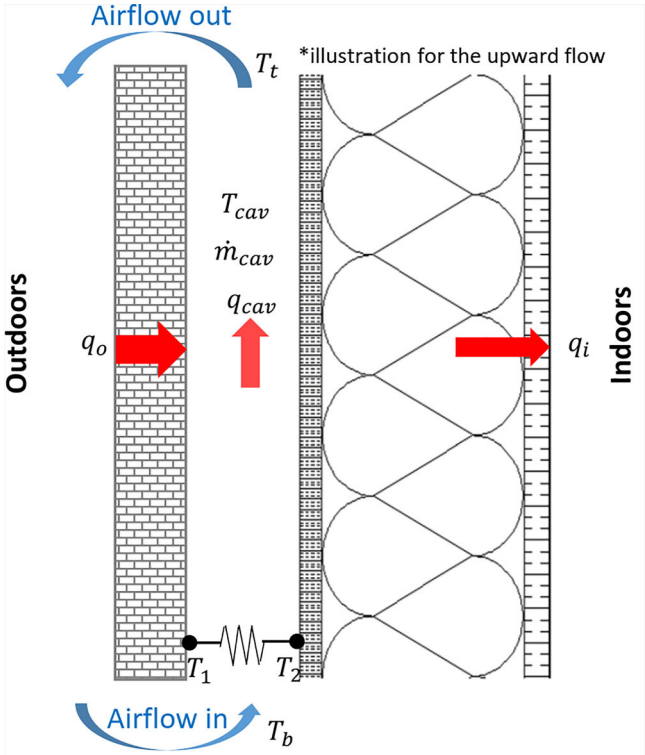

Fig. 7. *Apparent thermal resistance* ($R_{cav,app}$) based on the energy balance (Method 2) with q_i determined based on the energy balance to account for ventilated airflow heat transfer with the use of an *apparent* thermal resistance for the cavity (summer condition is shown) (source: Authors).

ventilation air is accounted for in the *effective thermal resistance* determined as described below, and it can be used in the context of conventional design of wall assemblies that include ventilated air cavities. The definition per Method 3 is straightforward since it employs a well-established definition of total thermal resistance of the wall assembly and a simple additive rule. Also, the use of $R_{cav,eff}$ is limited to specific cases (i.e., no solar flux effect) because the inclusion of solar energy can cause the effective thermal resistance to assume large negative or positive values due to the varying conditions under which solar gain can have positive (reduce heating loads) or negative (increase cooling loads) effects; thus, one should use it with care.

The details of each definition are discussed in the following subsections. The input values such as heat flux, temperatures of the surfaces, indoor and outdoor temperatures were calculated based on the energy balance using the numerical code that has already been presented in the previous section.

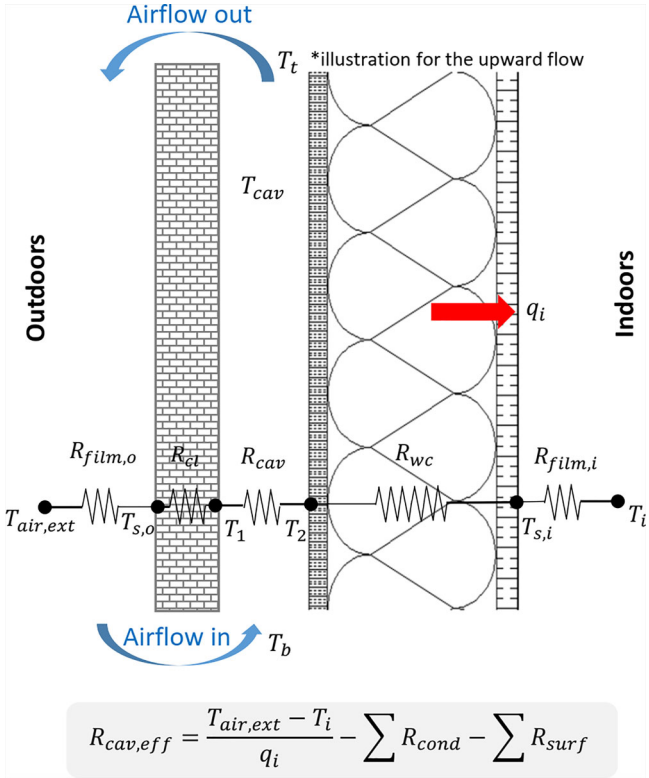

Fig. 8. *Effective thermal resistance* ($R_{cav,eff}$) based on the linearized network of thermal resistances (Method 3) with q_i determined based on the energy balance to account for ventilated airflow heat transfer with the use of an *effective* thermal resistance for the cavity (summer condition is shown) (source: Authors).

Definition of the thermal resistance of the air gap considering a non-linear network of thermal resistances (Method 1)

The network of thermal resistances in the ventilated cavity is illustrated in Figure 9. As shown, the network of thermal resistances inside the air gap is non-linear and can be presented either as a triangular (Δ) connection or a star (Y) connection (Stevenson 1975; Kennelly 1899).

In the triangular (Δ) connection, $R_{cav,conv,1}$ represents the convective thermal resistance of the left cavity surface,$R_{cav,conv,2}$ indicates the convective thermal resistance of the right cavity surface, and $R_{rad,12}$ shows the radiative thermal resistance between two cavity surfaces (Ciampi, Leccese, and Tuoni 2003). In the star (Y) connection, r_1 indicates the surface thermal resistance of the left cavity wall, r_2 shows the surface thermal resistance of the right cavity wall, and R represents the thermal resistance for the heat flux absorbed by the fluid in the air duct (Ciampi, Leccese, and Tuoni 2003). The same Δ-Y transformation has been introduced by Ciampi, Leccese, and Tuoni (2003) and the corresponding resistances defined as:

$$r_1 = \frac{R_{cav,conv,1} \cdot R_{rad,12}}{R_{cav,conv,1} + R_{cav,conv,2} + R_{rad,12}} \quad (42)$$

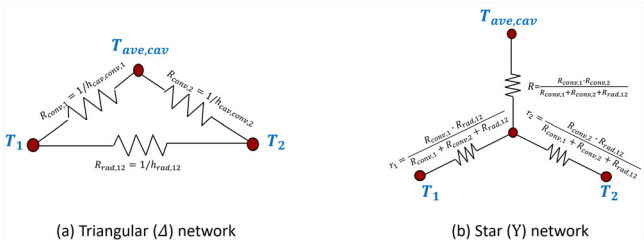

Fig. 9. The networks of thermal resistances for heat transfer in the vertical ventilated air-space (a) triangular network (b) star network (source: Authors).

$$r_2 = \frac{R_{cav,\,conv,\,2} \cdot R_{rad,\,12}}{R_{cav,\,conv,\,1} + R_{cav,\,conv,\,2} + R_{rad,\,12}} \tag{43}$$

$$R = \frac{R_{cav,\,conv,\,1} \cdot R_{cav,\,conv,\,2}}{R_{cav,\,conv,\,1} + R_{cav,\,conv,\,2} + R_{rad,\,12}} \tag{44}$$

The total thermal resistance of the entire wall assembly can be expressed according to the following equation (Ciampi, Leccese, and Tuoni 2003):

$$R_{total} = R_{film,\,o} + R_{cl} + r_1 + r_2 + R_{wc} + R_{film,\,i} \tag{45}$$

The above formulation for the total thermal resistance R_{total} of the ventilated wall assembly with a term of $(r_1 + r_2)$ has been acknowledged in other research publications. Patania et al. (2010) performed CFD simulations to obtain the velocity and temperature profiles in a ventilated façade. The thermal resistance of the entire assembly was defined similarly to the equation given by Ciampi, Leccese, and Tuoni (2003). Gagliano et al. (2014) used CFD to investigate the flow and thermal behavior of four types of ventilated facades and explicitly expressed that the convective and the radiative heat transfer within the ventilated cavity can be represented with an acceptable level of accuracy considering the same equations given by Ciampi, Leccese, and Tuoni (2003). A ventilated wall component was constructed in actual scale and tested under the real weather conditions (summer) in an outdoor test cell by Dimoudi, Androutsopoulos, and Lykoudis (2016). The same formulations, as expressed by Ciampi, Leccese, and Tuoni (2003), have been presented in this research work. A simplified dynamic thermal network model was established by Xiong, Yu, and Yang (2015) to obtain the thermal performance of the hollow block ventilated wall, which physically can be considered as a ventilated cavity. They introduced the same Δ-Y network for one representative ventilated hollow brick. A similar process was followed by Yu et al. (2017) using an experimental approach, and the corresponding heat transfer model was validated against measurements. The heat transfer model established for the hollow block ventilated wall was reasonable with a high degree of accuracy. According to the results, this model can be used to predict the surface temperature of the hollow block ventilated wall and the heat flux removed by the airflow in the cavity for performance evaluation. Although the thermal resistance of the ventilated cavity has not been explicitly expressed in the mentioned above studies, the corresponding formula of the thermal resistance of the ventilated air gap can be extracted from Equation (45) as:

$$R_{cav} = r_1 + r_2 \tag{46}$$

By defining the expressions for r_1 and r_2, the above equation can be re-written as:

$$R_{cav} = \frac{\left(\frac{1}{h_{cav,\,conv,\,1}} + \frac{1}{h_{cav,\,conv,\,2}}\right) \cdot \frac{1}{h_{rad,\,12}}}{\left(\frac{1}{h_{cav,\,conv,\,1}} + \frac{1}{h_{cav,\,conv,\,2}}\right) + \frac{1}{h_{rad,\,12}}} \tag{47}$$

As described above, this method might not be straightforward enough for use in practice because the thermal resistance for the cavity, as determined by Method 1 only has relevance to wall assemblies that are evaluated using this method, which explicitly and separately accounts for heat transfer caused by ventilation air. Therefore, additional methods of expressing apparent and effective thermal resistance of the ventilated air gap are presented in the next sections.

Definition of the apparent thermal resistance of the air gap considering energy balance (Method 2)

In Method 2, the thermal resistance is formulated using a common definition of the apparent thermal resistance, which is the ratio of the temperature difference between two walls of the ventilated air gap over the heat flux that is passing toward the wall core:

$$R_{cav,\,app} = \frac{\Delta T_{1-2}}{q_o + \dot{m} C_p \Delta T_{t-b}} = \frac{\Delta T_{1-2}}{q_{wc}} \tag{48}$$

The numerator in the Equation (48) is the temperature difference of the ventilated cavity walls, and the denominator is the summation of heat flux entering/leaving the exterior side of the building envelope (q_o) and the enthalpy of the flow passing through the ventilated cavity ($\dot{m} C_p \Delta T_{t-b}$). It needs to be mentioned that by applying the energy balance to the entire geometry, the summation of the heat flux passing through the *exterior* side of the building envelope (q_o) and the enthalpy flow in the ventilated cavity ($\dot{m} C_p \Delta T_{t-b}$) is always equal to the heat flux entering/leaving the interior side of the building envelope (q_i) as provided by the Equation (49). The sign of the right-hand side term may change according to the direction of the heat flow.

$$q_o + \dot{m} C_p \Delta T_{t-b} = q_i \tag{49}$$

On its turn, the heat flux entering/leaving the interior side of the building envelope (q_i) based on energy balance in the steady-state condition is equal to the heat flux passing through the wall core due to conduction (q_{wc}). Thus, q_i can be defined by knowing the temperature difference across the wall core and its thermal resistance due to conduction (Aelenei 2006):

$$q_i = q_{wc} = \frac{(T_2 - T_{s,\,i})}{R_{wc}} \tag{50}$$

Definition of the effective thermal resistance of the air gap considering the linear network of thermal resistances (Method 3)

Developing a simplified method to formulate the thermal resistance of the ventilated air gap that can be easy to apply

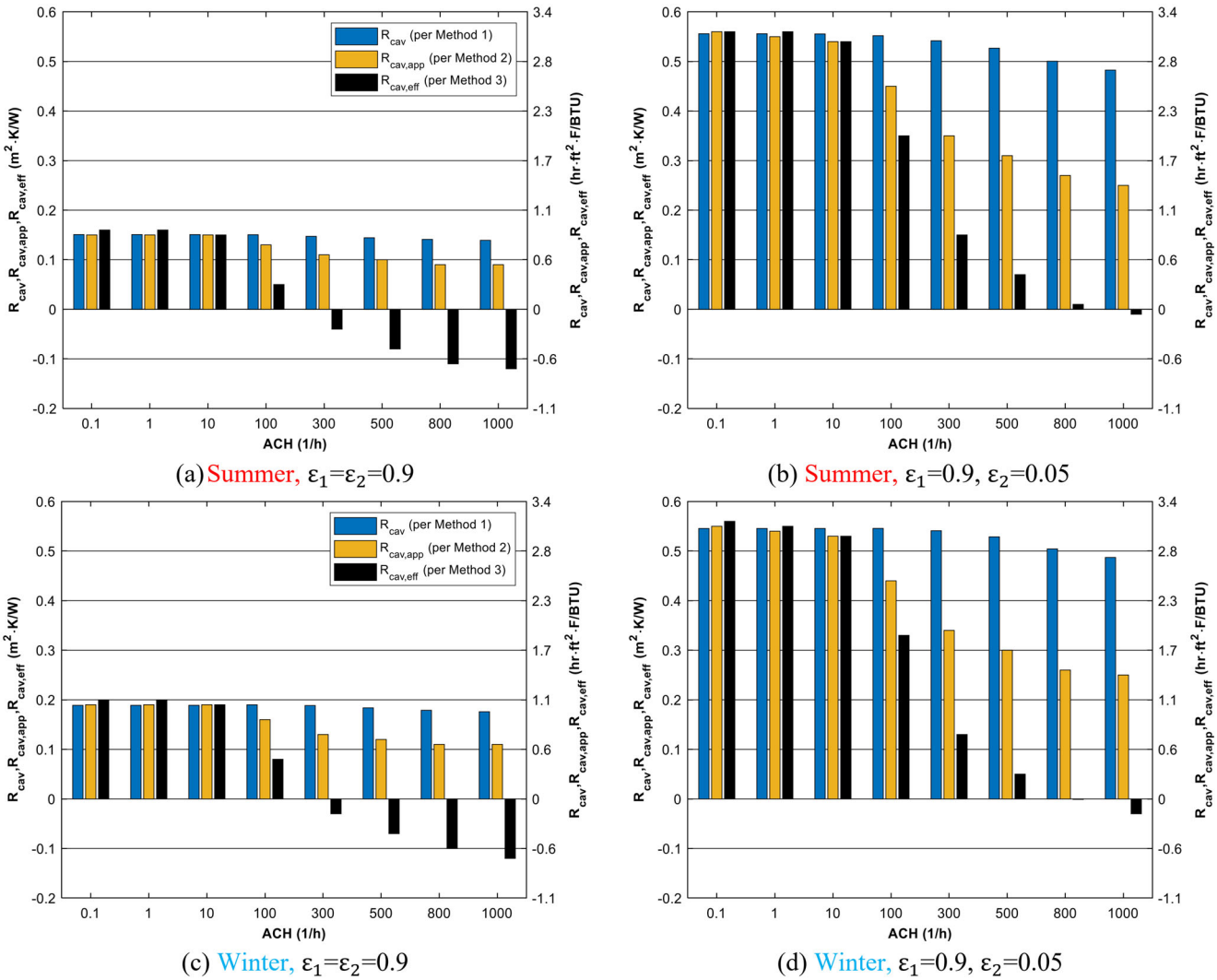

Fig. 10. Comparison of thermal resistance of the ventilated cavity behind brick cladding based on different definitions at I = 0 W/m^2.

in practice is one of the main objectives of the present work. A practical method defined in the current subsection uses a well-established approach of taking an effective thermal resistance of the wall assembly by summing up thermal resistances of separate wall elements. Although the actual network of thermal resistances of a ventilated wall assembly is not linear due to the heat flow removed by the airflow, the *linearization* of the thermal resistance is imposed in this method to make the calculation procedure as close as possible to the conventional practice.

The total thermal resistance of the wall assembly (R_{total}) can be obtained by following the well-established definition presented in Equation (51) in which the ratio of the temperature difference between the outside and inside air divided by the heat flux passing through the wall core (q_i). The thermal resistance of the entire wall assembly can also be expressed via a series of thermal resistances across the wall, as presented in Equation (52), which is a common procedure used in practice.

$$R_{total} = \frac{T_{air,ext} - T_i}{q_i} \tag{51}$$

$$R_{cav,eff} = R_{total} - \left(\sum R_{cond} + \sum R_{film}\right) \tag{52}$$

The *effective* thermal resistance of the ventilated cavity can be extracted from the calculated value (R_{total}) by subtracting the thermal resistances of the wall core and cladding due to conduction (Equation (53)) and the film resistance of the interior and exterior surfaces (Equation (54)).

$$\sum R_{cond} = R_{cl} + R_{wc} \tag{53}$$

$$\sum R_{film} = R_{film,i} + R_{film,o} \tag{54}$$

The film thermal resistances can be determined using tabulated data provided in ASHRAE Standard 90.1. The values for the thermal resistances of the cladding and wall core can be determined by knowing the thermal properties of materials by assuming that walls are impermeable: (i) define

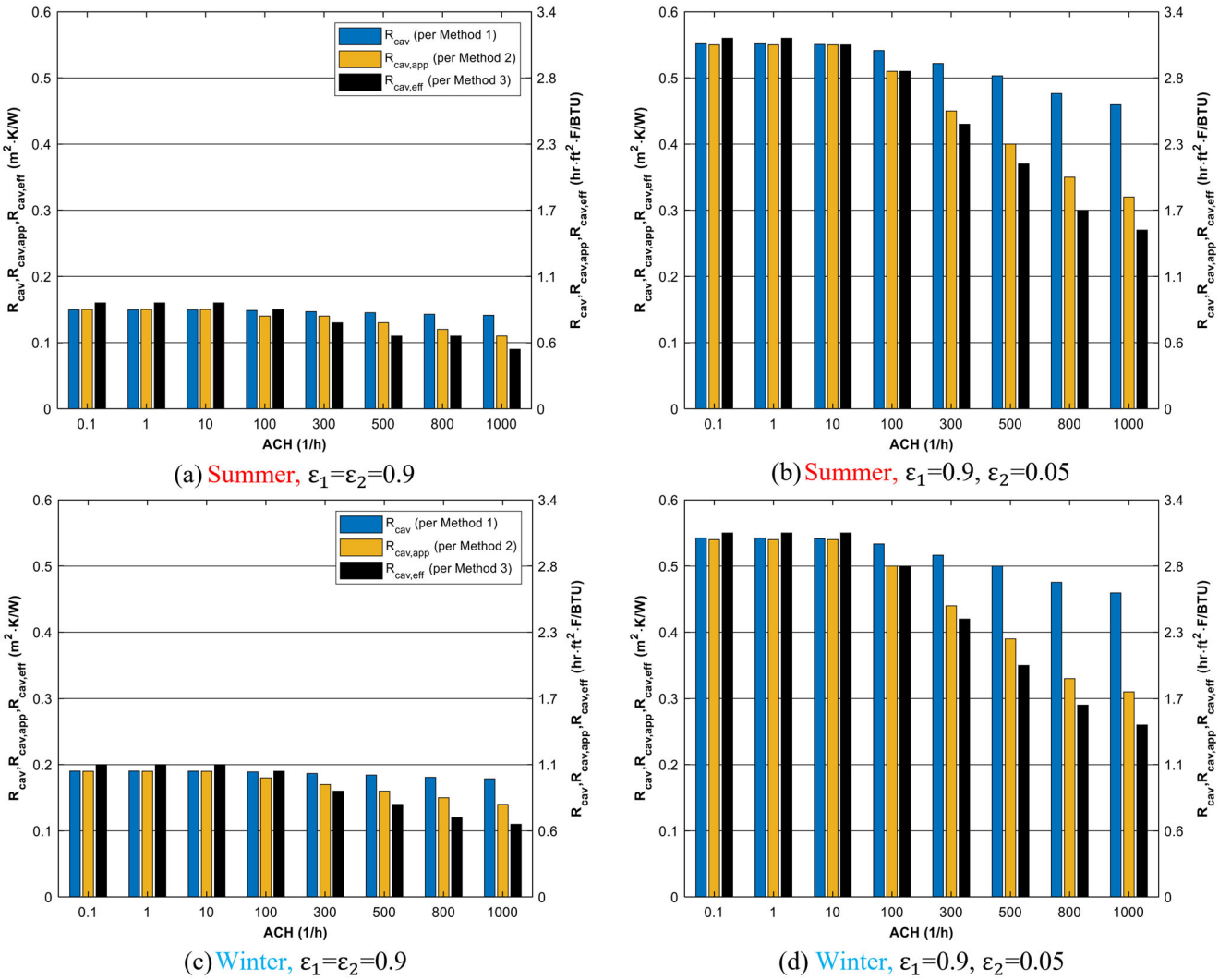

Fig. 11. Comparison of thermal resistance of the ventilated cavity behind vinyl siding cladding based on different definitions of methods at I = 0 W/m^2.

thermal resistance of the claddingR_{cl} by dividing the thickness of the cladding by its thermal conductivity; (ii) define thermal resistance of the wall coreR_{wc} by dividing the thickness of the wall core by its thermal conductivity.

Comparison of the methods and discussion

The results on the thermal resistance of the ventilated air gap (called cavity thermal resistance based on Method 1, *apparent* based on Method 2, and *effective* based on Method 3) are compared in Figures 10 and 11 for the range of ACH from 0.1 1/h up to 1000 1/h at no solar effect ($I = 0$ W/m^2). The solar flux effect was not considered for a few reasons:

- First of all, the energy balance across the wall assembly presented in section 0 was simplified and did not consider the thermal mass of the wall materials. Thermal mass effects, especially in the brick veneer cladding, could have a profound effect on the temperature distribution across the assembly. Thus, thermal resistances calculated based on the definitions in the previous subsections can be used only for steady-state conditions with a certain accuracy.
- In addition to that, the conventional hot box method outlined in ASTM C1363-19 and used for rating the performance of the wall assembly is only appropriate for steady-state conditions and does not provide the possibility to test the solar flux effect. Thus, it is reasonable to consider only non-solar effect cases to modify the test method further.

General input parameters (thermo-physical properties, outdoor air temperature, *etc.*) are shown in Table 5. Two types of traditional external claddings (e.g., vinyl siding, brick veneer) incorporated with a ventilated cavity are considered. The value of the thermal conductivity of the wall core was taken as $k = 0.03$ BTU/hr· ft· F (0.06 W/m· K). For the considered k value, the corresponding thermal resistance

Table 5. Input parameters.

Symbol	Unit (IP; SI)	Value	
		Brick cladding	Vinyl Siding (PVC)
δ_{cl}	ft (m)	39.37 (0.12)	0.039 (0.012)
k_{cl}	BTU/(hr · ft · F) [W/(m · K)]	0.25 (0.43)	0.11 (0.19)
δ_{wc}	ft (m)	0.3 (0.16)	0.3 (0.16)
k_{wc}	BTU/(hr · ft · F) [W/(m · K)]	0.02, 0.03, 0.10 (0.03, 0.06, 0.18)	
d_{cav}	ft (m)	0.08 (0.025)	0.030 (0.009)
$T_{air,ext}$	°F (°C)	Winter 32 (0), Summer 95 (35)	
V_{wind}	ft/s (m/s)	16.4 (5)	
θ	Degree	0	
ε_1	–	0.9	
ε_2	–	0.9 and 0.05	
H	ft (m)	9.84 (3)	
w	ft (m)	3.28 (1)	

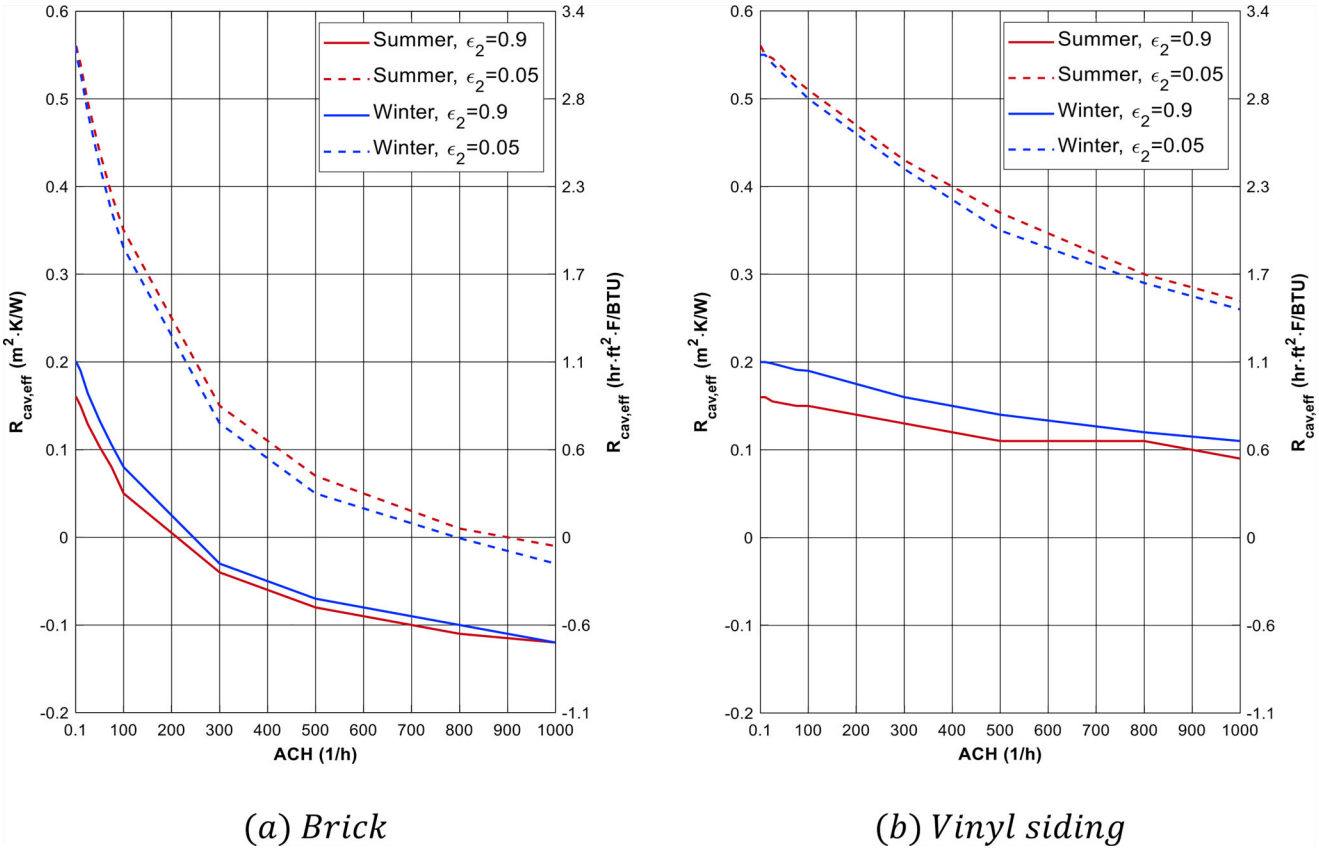

Fig. 12. Effective thermal resistance of the ventilated cavity at I = 0 W/m^2.

of the wall core (R_{wc}) is 15.16 hr· ft^2· F/BTU (2.67 m^2· K/W). Based on the physical properties of the wall assemblies, the thermal resistance of the brick cladding due to conduction is R_{br} =1.59 hr· ft^2· F/BTU (0.28 m^2· K/W) and for vinyl siding is R_{vs} = 0.36 hr· ft^2· F/BTU (0.063 m^2· K/W). The film resistances are taken from the tabulated data in ASHRAE Standard 90.1 are the following: $R_{film,o}$ =0.2 hr· ft^2· F/BTU (0.03 m^2· K/W) for the exterior surfaces and $R_{film,i}$ =0.7 hr· ft^2· F/BTU (0.12 m^2· K/W) for the interior vertical wall. The effect of the presence of the reflective insulation on the cavity surface adjacent to the wall core (ε_2) is also investigated by varying the emissivity of the surface from 0.9 to 0.5. Two outdoor temperatures that represent the summer and winter conditions in fixed wind speed are considered (Table 5).

Figures 10 and 11 show results for each analysis wall and season. According to the results, by increasing the ACH, the thermal resistance of the air-space decreases per all methods.

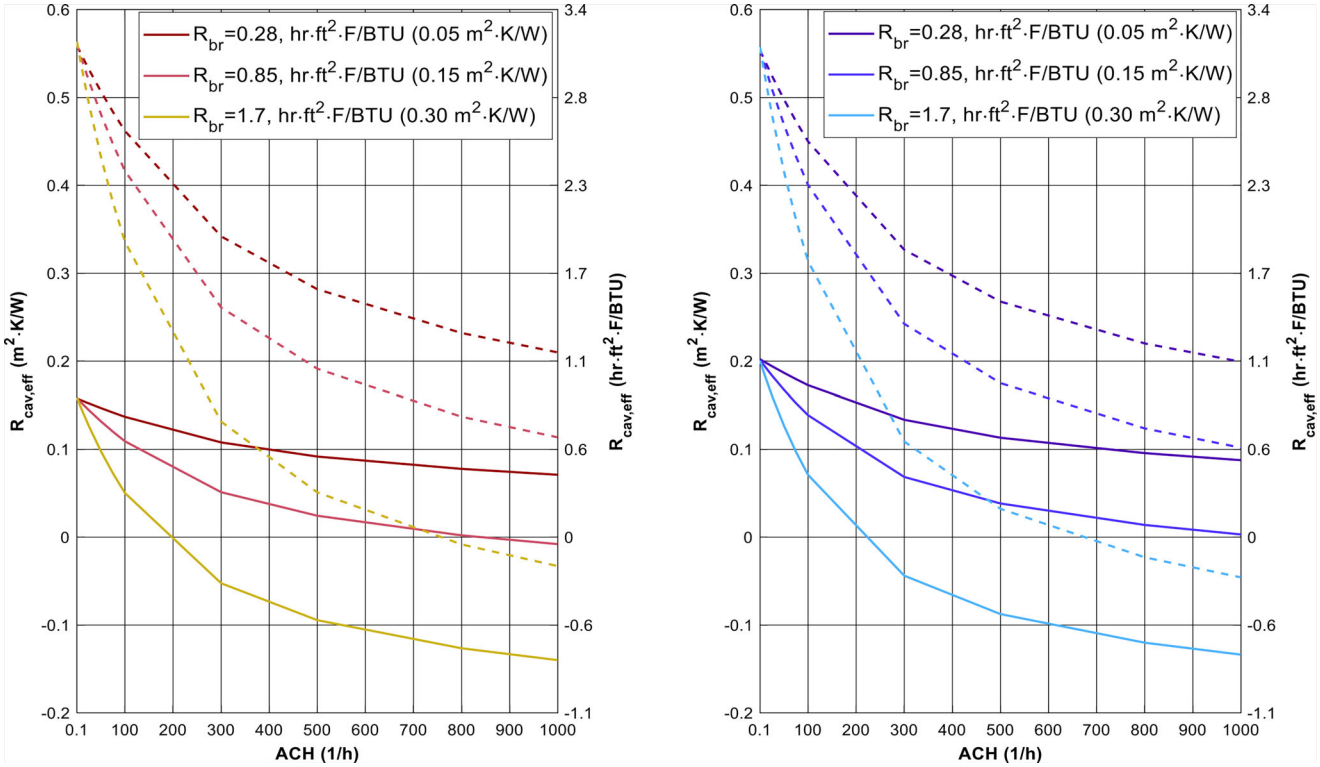

Fig. 13. Effective thermal resistance of the ventilated cavity behind brick cladding with different R-values of the cladding at I = 0 W/m^2. (Solid lines: $\varepsilon_1 = \varepsilon_2 = 0.9$; dashed lines: $\varepsilon_1 = 0.9$ & $\varepsilon_2 = 0.05$.)

Once the ACH increases, the mean velocity in the cavity, as well as the convective heat transfer coefficient inside the cavity, becomes higher which turns the thermal resistance per Method 1 to decrease. On the other hand, the heat flow in the cavity increases in higher ACH values which consequently increases the temperature gradient within the wall core and eventually makes the thermal resistance lower per Method 2 and Method 3. The thermal resistances characterized based on the boundary conditions inside the cavity per Method 1 and Method 2 are closer in both cladding types. In the case of vinyl siding, the values of methods 2 and 3 are closer than the case of the brick wall. This is because the thermal resistance value of vinyl siding is lower than brick, which has less effect on thermal resistance.

Considering the illustrations in Figures 10 and 11, the values of $R_{cav,app}$ are quite close to the values of R_{cav}. The difference between the thermal resistance per Method 1 and Method 2 is higher (on average, 6% in the brick wall and 10% in the vinyl siding) when the reflective insulation is used. In the case of brick cladding, the difference between the *effective* thermal resistance ($R_{cav,eff}$ and the other two methods become higher when the ACH values increase (can reach up to 200% when Method 2 is compared with Method 3). In contrast, there is a small difference between all three methods in the case of vinyl siding cladding. This is the result of the effect of the external cladding—a thin layer of vinyl siding conducts heat well, which results in a smaller temperature gradient through the entire assembly compared to brick cladding. The temperature gradient through the wall core also does not change remarkably in the case of using vinyl siding, which makes the thermal resistance of the cavity obtained from Method 2 close to the calculated values from Method 3. The results show that the difference between the two pairs of selected thermal resistances of the air gap increases at higher ACH values. This trend is due to the dependence of Method 2 and Method 3 on the value of the heat flux passing through the wall core (q_i). In other words, once the airflow rate behind the external claddings increases, the temperature gradient in the wall core ($T_2 - T_{s,int}$), and consequently, the heat flux entering/leaving the interior side of the building becomes higher, which eventually affects the thermal resistance of the ventilated cavity.

Since the effective thermal resistance $R_{cav,eff}$ defined by Method 3 seems to be convenient for conventional engineering analysis and is the basis for how thermal resistances are applied for energy code compliance, further analysis will be carried out for effective thermal resistance only. Figure 12 shows the variation of $R_{cav,eff}$ for two types of external claddings. According to the results, by increasing the ACH value, the $R_{cav,eff}$ will be more influenced in the case of using reflective insulation in the cavity (the slope of the curves is greater in $\varepsilon_2 = 0.05$ cases than the $\varepsilon_2 = 0.9$ cases). This is mainly due to the temperature gradient in the wall core, which is higher in the case of using the reflective insulation. In the case of using a brick veneer, this temperature gradient caused by the reflective insulation becomes more significant compared with the vinyl siding. Moreover, there are some negative values of the effective thermal resistances in the case of using the brick wall. The negative values of $R_{cav,eff}$ are due to the smaller values of R_{tot} than the summation of the other terms (Equation

(52)). In contrast to the solid materials in which a negative thermal resistance is meaningless, negative values of the effective thermal resistance of a ventilated cavity can be interpreted as to its adverse contribution to the total thermal resistance of the assembly. According to the below figure, $R_{cav,eff}$ decreases as ACH increases, and the degree of $R_{cav,eff}$ drop depends on the ACH value. Ventilation airflow in the air cavity effectively *off-sets* or *diminishes* the thermal resistance contribution of the cladding to the overall wall assembly, and the cladding thermal resistance no longer fully contributes to the simple linearized network of thermal resistances as defined by the Method 3 depiction of *an effective thermal resistance* for a ventilated air-space. Thus, the magnitude of an effective thermal resistance of a ventilated air-space as defined by Method 3 is dependent on the thermal resistance of the cladding. External claddings having a small thermal resistance, for example, a thin vinyl siding having R_{vs}=0.36 hr·ft^2·F/BTU (0.06 m^2·K/W) shown in Figure 12(b), have a smaller thermal resistance contribution to the overall wall assembly. For external claddings having greater thermal resistance, for example, brick veneers that can have R-value in the range R_{br}= 0.28 hr·ft^2·F/BTU (0.05 m^2·K/W) to R_{br}= 1.70 hr·ft^2·F/BTU (0.30 m^2·K/W), the increase in ventilation rate with no direct solar gain in summer can results in an increase in the thermal resistance penalty, as shown in Figure 13. Admittedly, at a certain ACH level for a given cladding thermal resistance, even a negative *effective thermal resistance* can occur. Thus, the effective thermal resistance of the air-space per Method 3 does not represent a physical quantity, but it is necessary to align the thermal performance of the assembly as depicted by Method 3 with the more complex and physically correct analysis of the assembly as represented by Method 1. Hence, in the context of Method 3, it is called an *effective thermal resistance* in this study.

Conclusion

The presence of a ventilated air-space behind external cladding systems can affect the thermal performance of the wall assembly. Several factors, such as air exchange rate, external cladding type, seasonal variation, and presence of reflective insulation, can influence the thermal resistance of the air-space. Because the thermo-hydrodynamic parameters in the cavity change dynamically as a function of the aforementioned factors, formulating the actual thermal resistance of the cavity was challenging. To address this challenge, a detailed steady-state analysis of energy balance in the wall assembly was performed, and plausible definitions of the thermal resistance of a ventilated air cavity behind vertical facades were defined in this paper. Three definitions were introduced to describe the thermal characteristics of the air in the air gap. The first method was based on the non-linear network of thermal resistances of different layers in the wall structure. Due to the complexity of using this method in practice and the necessity to consider the thermal mass effect for the cladding and the wall core, two other methods were also introduced. The *apparent* and *effective* thermal resistances of the ventilated cavity were defined within these methods. The *apparent* thermal resistance ($R_{cav,app}$) was defined based on energy balance and requires knowledge of surface temperatures of the cavity. It should be noted that the temperatures of the cavity surfaces could be measured using temperature sensors such as thermocouples on each surface. The *effective* thermal resistance ($R_{cav,eff}$) was defined based on a linear network of thermal resistances in an analogy with a closed cavity. Since the effect of solar flux and thermal inertia were not considered in the simulations, all definitions should be used only for steady-state and non-solar conditions. The definition of *effective* thermal resistance was defined as the most convenient way of characterizing thermal resistance of the air gap from a practical point of view, accounting that the linearized network of thermal resistances of building components is the basis for energy code compliance applications.

According to the results, the values of the $R_{cav,eff}$ could be in the range from 0.28 hr·ft^2·F/BTU (0.05 m^2·K/W) to 3.12 hr·ft^2·F/BTU (0.55 m^2·K/W) in the case of the wall assembly with the brick cladding for ACH values up to 100 1/h. These values were remarkable when compared with thermal resistances of the remaining parts of the assembly: the cladding has R_{br}=1.59 hr·ft^2·F/BTU (0.28 m^2·K/W), the wall core has R_{wc}=15.10 hr·ft^2·F/BTU (2.66 m^2·K/W), and the sum of film resistances is $\sum R_{film}$=0.91 hr·ft^2·F/BTU (0.16 m^2·K/W)). Interestingly, the air-space could be able to resist the incoming or outgoing heat flux from indoors even more than the external cladding when reflective insulation is used on one of the sides of the cavity. Even though thermal resistance of the cavity $R_{cav,eff}$ decreased as ACH increased, the variation of $R_{cav,eff}$ for brick veneer case at ACHs up to 100 1/h is still considerable: (i) equal to 0.57 hr·ft^2·F/BTU (0.1 m^2·K/W) when reflective insulation was not used, and (ii) equal to 1.14 hr·ft^2·F/BTU (0.2 m^2·K/W) when reflective insulation was considered on the outer face of the wall core. The same trend was observed for the case of the wall assembly with vinyl siding in the range of ACH up to 1000 1/h. The aforementioned values correspond to the zero solar flux conditions. In the case of exposing the cladding to solar radiation, it is expected that the thermal resistance of the ventilated air gap can vary even more. Therefore, the results of this study confirmed that the air-space could have a noticeable contribution to the thermal performance of the ventilated wall assembly.

While the steady-state solution was sufficient to show the main effects of the ventilated air gap on the thermal performance of the wall assembly, it is recommended to develop a theoretical solution that can include the transient effects of the outdoor and indoor parameters on the dynamic performance of the wall assembly with actual non-zero solar flux conditions. Moreover, detailed simulations of thermal bridges, airflow blockage, and re-circulation zones due to the presence of studs, junctions, and anchors can be performed to improve the evaluation of the thermal performance of the assembly. Furthermore, some studies demonstrated that higher ventilation rates in the cavity can enhance its drying potential. This would alternatively result in a lower thermal resistance of the air-space for energy conservation purposes. Thus, further studies are needed to find a tradeoff for the ventilation rate in the cavity and evaluate an optimized value for the air change rate in the ventilated air-spaces behind external claddings under different conditions.

Nomenclature

Symbol	Unit IP (SI)	Definition
α	–	Absorption coefficient of the external surface
σ	–	Boltzmann constant
ρ	lb/ft^3 (kJ /m^3)	Density
μ	lbf· s/ft^2 (Pa· s)	Dynamic viscosity
ε	–	Emissivity
δ	ft (m)	Thickness
C_p	BTU/lb·°F (kJ· kg/K)	Specific heat
d	in (mm)	Thickness
F	–	View factor
h	BTU/hr· ft^2·°F (W/m^2· K)	Heat transfer coefficient
H	ft (m)	Height
I	W/m^2	Incident solar radiation
k	BTU/hr· ft· F (W/m· K)	Thermal conductivity
q	BTU/hr· ft^2 (W/m^2)	Heat flux
r	hr· ft^2· F / BTU (m^2· K/W)	Surface thermal resistance
R	hr· ft^2· F / BTU (m^2· K/W)	Thermal resistance
T	°F (°C)	Temperature
u	ft/s (m/s)	Mean velocity
V	ft/s (m/s)	Speed
w	ft (m)	Width

Subscripts

Symbol	Definition
1	Left surface of the ventilated cavity
2	Right surface of the ventilated cavity
air	Air
app	Apparent
ave	Average
b	Bottom
br	Brick
cav	Cavity
cl	Cladding
cond	Conduction
conv	Convective
eff	Effective
en	Entrance
eq	Equivalent
ext	Exterior
film	Film
i	Indoor
int	Interior
m	Mean
o	Outdoor
r	Radiation
rad	Radiative
s	Surface
sk	Sky
t	Top
vs	Vinyl siding
wc	Wall core
wind	Wind

Acknowledgments

The authors acknowledge the Project Monitoring Subcommittee members (M. Bianchi, J. Crandell, H. Ge, and P.C.T. Velasco) for their constructive feedback during the study.

Funding

This study was a part of ASHRAE RP-1759 sponsored by the TC 4.4 committee (Building Materials and Building Envelope). It also received financial support from École Polytechnique Fédérale de Lausanne (EPFL).

References

Aelenei, L. 2006. Thermal performance of naturally ventilated cavity walls. 195. Ph.D. Thesis. Universidade Técnica de Lisboa.

ASHRAE. 2009. *Handbook—Fundamentals (SI edition)*. Atlanta, Georgia: American Society of Heating, Refrigerating and Air-Conditioning Engineers, Inc.

ASHRAE Standard. 2016. ASHRAE Standard 90.1. Energy standard for buildings except low-rise residential buildings.

ASTM 1363-05. 2009. Thermal performance test report. Rendered to E.I. DUPONT DE NEMOURS AND COMPANY.

Baldinelli, G. 2010. A methodology for experimental evaluations of low-e barriers thermal properties: Field tests and comparison with theoretical models. *Building and Environment* 45 (4):1016–24. doi:10.1016/j.buildenv.2009.10.009

Balocco, C. 2002. A simple model to study ventilated facades energy performance. *Energy and Buildings* 34 (5):469–75. doi:10.1016/S0378-7788(01)00130-X

Balocco, C. 2009. Transient simulation of a naturally ventilated façade in a Mediterranean climate. *Comsol Conference* 2009:1–5.

Bekkouche, S. M. A., T. Benouaz, M. K. Cherier, M. Hamdani, M. R. Yaiche, and N. Benamrane. 2013. Thermal resistances of air in cavity walls and their effect upon the thermal insulation performance. *International Journal of Energy and Environment* 4 (3):459–66.

Buratti, C., D. Palladino, E. Moretti, and R. Di Palma. 2018. Development and optimization of a new ventilated brick wall: CFD analysis and experimental validation. *Energy and Buildings* 168:284–97. doi:10.1016/j.enbuild.2018.03.041

Ciampi, M., F. Leccese, and G. Tuoni. 2003. Ventilated facades energy performance in summer cooling of buildings. *Solar Energy* 75 (6): 491–502. doi:10.1016/j.solener.2003.09.010

Desjarlais, A. O., and D. W. Yarbrough. 1991. Prediction of the thermal performance of single and multi-air-space reflective insulation materials. In *Insulation materials: Testing and applications*. ASTM International.

Dimoudi, A. C., A. V. Androutsopoulos, and S. P. Lykoudis. 2016. Experimental study of the cooling performance of a ventilated wall. *Journal of Building Physics* 39 (4):297–320. doi:10.1177/1744259114546282

Duffie, J. A., and W. A. Beckman. 2013. *Solar engineering of thermal processes*. 4th ed.

EXOVA Test Report. 2011. Thermal performance study for foam sheathing coalition. Report No. 10 06-M0211-FSC.

Falk, J., and K. Sandin. 2013. Ventilated rainscreen cladding: Measurements of cavity air velocities, estimation of air change rates and evaluation of driving forces. *Building and Environment* 59:164–76. doi:10.1016/j.buildenv.2012.08.017

Feng, G., S. Sha, and X. Xu. 2016. Analysis of the building envelope influence to building energy consumption in the cold regions. *Procedia Engineering* 146:244–50. doi:10.1016/j.proeng.2016.06.382

Finch, G., and J. Straube. 2007. Ventilated wall claddings: Review, field performance, and hygrothermal modeling. Thermal Performance of Exterior Envelopes of Whole Buildings X International Conference.

Gagliano, A., F. Patania, A. Ferlito, F. Nocera, and A. Galesi. 2014. Computational fluid dynamic simulations of natural convection in ventilated facades. *Intech Open* 2:64.

Gagliano, A., F. Nocera, and S. Aneli. 2016. Thermodynamic analysis of ventilated façades under different wind conditions in summer period. *Energy and Buildings* 122:131–9. doi:10.1016/j.enbuild.2016.04.035

Holman, P. J. 1991. *Heat transfer*. New York: McGraw-Hill.

ISO 6946. 2007. Building components and building elements—Thermal resistance and thermal transmittance-calculation method.

Kennelly, A. E. 1899. Equivalence of triangles and three-pointed stars in conducting networks. *Electrical World and Engineer* 34:413–4.

Langmans, J., and S. Roels. 2015. Experimental analysis of cavity ventilation behind rainscreen cladding systems: A comparison of four measuring techniques. *Building and Environment* 87:177–92. doi:10.1016/j.buildenv.2015.01.030

Manuel, V., S. Francés, E. José, S. Escriva, J. Manuel, P. Ojer, E. Bannier, V. Cantavella, and G. Silva. 2013. Modeling of ventilated facades for energy building simulation software. *Energy and Buildings* 65:419–28. doi:10.1016/j.enbuild.2013.06.015

Mathes, R., J. Blumenberg, and K. Keller. 1990. Radiative heat transfer in insulations with random fibre orientation. *International Journal of Heat and Mass Transfer* 33 (4):767–70. doi:10.1016/0017-9310(90)90174-S

Meyer, B., M. Spinu, T. Weston, and H. Kuhlman. 2019. Impact of low-E WRB facing an air cavity on the R-value of a wall system. *ASHRAE* 11:63–7.

NBCC. 2005. *National Building Code of Canada*, 12th ed. Ottawa: National Research Council of Canada.

Nusselt, W., and W. Jurges. 1922. Die kuhlung einer ebenen wand durch einen luftstrom (The cooling of a plane wall by an air flow). *Gesundheits-Ingenieur* 52 (45):641–2.

Patania, F., A. Gagliano, F. Nocera, A. Ferlito, and A. Galesi. 2010. Thermofluid-dynamic analysis of ventilated facades. *Energy and Buildings* 42 (7):1148–55. doi:10.1016/j.enbuild.2010.02.006

Rahiminejad, M., and D. Khovalyg. 2021. Review on expected ventilation rates in the ventilated cavity behind traditional cladding systems. *Building and Environment* 190:107538. doi:10.1016/j.buildenv.2020.107538

Richman, R. C., and K. D. Pressnail. 2009. A more sustainable curtain wall system: Analytical modeling of the solar dynamic buffer zone (SDBZ) curtain wall. *Building and Environment* 44 (1):1–10. doi:10.1016/j.buildenv.2008.01.006

Robinson, H. E., F. J. Powlitch, and R. S. Dill. 1954. *The thermal insulating value of airspaces*. Housing and Home Finance Agency, Housing Research Paper 32, U.S. Government Printing Office, Washington, D.C.

Saber, H. 2012. Investigation of thermal performance of reflective insulations for different applications. *Building and Environment* 52:32–44. doi:10.1016/j.buildenv.2011.12.010

Saber, H. 2013a. Practical correlation for thermal resistance of horizontal enclosed air-spaces with downward heat flow for building applications. *Journal of Building Physics* 37 (4):403–35. doi:10.1177/1744259113498473

Saber, H. 2013b. Thermal performance of wall assemblies with low emissivity. *Journal of Building Physics* 36 (3):308–29. doi:10.1177/1744259112450419

Schumacher, C. J., D. G. Ober, J. F. Straube, and A. P. Grin. 2013. Development of a new hot box apparatus to measure building enclosure thermal performance. Thermal Performance of the Exterior Envelopes of Whole Buildings—12th International Conference, Clearwater, Florida, USA.

Shehadi, M. 2018. Energy consumption optimization measures for buildings in the Midwest regions of USA. *Buildings* 8 (12):170. doi:10.3390/buildings8120170

Skoplaki, E., and J. A. Palyvos. 2009. Operating temperature of photovoltaic modules: A survey of pertinent correlations. *Renewable Energy* 34 (1):23–9. doi:10.1016/j.renene.2008.04.009

Straube, J. 1998. Moisture control and enclosure wall systems. *University of Waterloo* (January 1998).

Straube, J., and G. Finch. 2009. Ventilated wall claddings: Review, field performance, and hygrothermal modeling. Research Report-0907, Building Science Press.

Stevenson, W. 1975. *Elements of power system analysis*. 3rd ed. New York: McGraw Hill.

Tariku, F., and E. Iffa. 2019. Empirical model for cavity ventilation and hygrothermal performance assessment of wood frame wall systems: Experimental study. *Building and Environment* 157 (April):112–26.

Van Belleghem, M., M. Steeman, A. Janssens, and M. De Paepe. 2015. Heat, air and moisture transport modelling in ventilated cavity walls. *Journal of Building Physics* 38 (4):317–49. doi:10.1177/1744259114543984

Xiong, C., J. Yu, and J. Yang. 2015. Study of the simplified dynamic thermal network model for the hollow block ventilated wall. *Procedia Engineering* 121:1304–11. doi:10.1016/j.proeng.2015.09.008

Yu, J., J. Huang, X. Xu, H. Ye, C. Xiong, J. Wang, and L. Tian. 2017. A semi-dynamic heat transfer model of hollow block ventilated wall for thermal performance prediction. *Energy and Buildings* 134:285–94. doi:10.1016/j.enbuild.2016.11.001